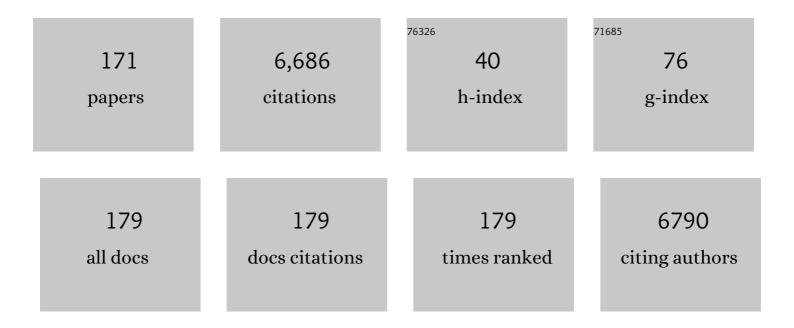
List of Publications by Year in descending order

Source: https://exaly.com/author-pdf/1208041/publications.pdf Version: 2024-02-01



MEINDAD REED

#	Article	lF	CITATIONS
1	Impact of Myocardial Fibrosis in Patients With Symptomatic Severe Aortic Stenosis. Circulation, 2009, 120, 577-584.	1.6	619
2	Long-Term Effects of Enzyme Replacement Therapy on Fabry Cardiomyopathy. Circulation, 2009, 119, 524-529.	1.6	422
3	Improvement of Cardiac Function During Enzyme Replacement Therapy in Patients With Fabry Disease. Circulation, 2003, 108, 1299-1301.	1.6	363
4	Absolute concentrations of high-energy phosphate metabolites in normal, hypertrophied, and failing human myocardium measured noninvasively with 31P-SLOOP magnetic resonance spectroscopy. Journal of the American College of Cardiology, 2002, 40, 1267-1274.	2.8	325
5	Low-Gradient Aortic Valve Stenosis. Journal of the American College of Cardiology, 2011, 58, 402-412.	2.8	265
6	The variation of morphological and functional cardiac manifestation in Fabry disease: potential implications for the time course of the disease. European Heart Journal, 2005, 26, 1221-1227.	2.2	214
7	Chronic nonbacterial osteomyelitis in childhood: prospective follow-up during the first year of anti-inflammatory treatment. Arthritis Research and Therapy, 2010, 12, R74.	3.5	171
8	Differences in Fabry Cardiomyopathy Between Female and Male Patients. JACC: Cardiovascular Imaging, 2011, 4, 592-601.	5.3	157
9	Elevated Cardiac Troponin T in PatientsÂWith Skeletal Myopathies. Journal of the American College of Cardiology, 2018, 71, 1540-1549.	2.8	150
10	Impact of Enzyme Replacement Therapy on Cardiac Morphology and Function and Late Enhancement in Fabry's Cardiomyopathy. American Journal of Cardiology, 2006, 97, 1515-1518.	1.6	141
11	Two-dimensional speckle tracking as a non-invasive tool for identification of myocardial fibrosis in Fabry disease. European Heart Journal, 2013, 34, 1587-1596.	2.2	125
12	Gene Mutations Versus Clinically Relevant Phenotypes. Circulation: Cardiovascular Genetics, 2014, 7, 8-16.	5.1	118
13	Relation of Burden of Myocardial Fibrosis to Malignant Ventricular Arrhythmias and Outcomes in Fabry Disease. American Journal of Cardiology, 2014, 114, 895-900.	1.6	112
14	Analysis of First-Pass and Delayed Contrast-Enhancement Patterns of Dysfunctional Myocardium on MR Imaging. American Journal of Roentgenology, 2000, 174, 1737-1740.	2.2	109
15	Prebolus quantitative MR heart perfusion imaging. Magnetic Resonance in Medicine, 2004, 52, 296-299.	3.0	103
16	Small-bowel MRI in children and young adults with Crohn disease: retrospective head-to-head comparison of contrast-enhanced and diffusion-weighted MRI. Pediatric Radiology, 2013, 43, 103-114.	2.0	96
17	Cardiac Systolic Rotation and Contraction Before and After Valve Replacement for Aortic Stenosis. American Journal of Roentgenology, 2002, 178, 953-958.	2.2	91
18	A new echocardiographic approach for the detection of non-ischaemic fibrosis in hypertrophic myocardium. European Heart Journal, 2007, 28, 3020-3026.	2.2	90

#	Article	IF	CITATIONS
19	Autoinflammatory bone disorders. Clinical Immunology, 2013, 147, 185-196.	3.2	86
20	Detection of myocardial viability by low-dose dobutamine cine MR imaging. Magnetic Resonance Imaging, 1999, 17, 1437-1443.	1.8	83
21	Concentrations of human cardiac phosphorus metabolites determined by SLOOP31P NMR spectroscopy. Magnetic Resonance in Medicine, 1999, 41, 657-663.	3.0	77
22	SElfâ€gated Non ontrastâ€Enhanced FUnctional Lung imaging (SENCEFUL) using a quasiâ€random fast Iowâ€angle shot (FLASH) sequence and proton MRI. NMR in Biomedicine, 2014, 27, 907-917.	2.8	69
23	Cardiac Magnetic Resonance Imaging Findings in 20-year Survivors of Mediastinal Radiotherapy for Hodgkin's Disease. International Journal of Radiation Oncology Biology Physics, 2011, 79, 1117-1123.	0.8	68
24	Optimization of automatic bolus tracking for timing of the arterial phase of helical liver CT. European Radiology, 2001, 11, 1396-1400.	4.5	63
25	Diagnostic value of MRI-based 3D texture analysis for tissue characterisation and discrimination of low-grade chondrosarcoma from enchondroma: a pilot study. European Radiology, 2018, 28, 468-477.	4.5	62
26	Chronic multifocal non-bacterial osteomyelitis in hypophosphatasia mimicking malignancy. BMC Pediatrics, 2007, 7, 3.	1.7	61
27	Varicella-zoster virus infections in immunocompromised patients - a single centre 6-years analysis. BMC Pediatrics, 2011, 11, 31.	1.7	61
28	Assessment of Myocardial Infarction in Humans with23Na MR Imaging: Comparison with Cine MR Imaging and Delayed Contrast Enhancement. Radiology, 2001, 221, 222-228.	7.3	57
29	The right ventricle in Fabry disease: natural history and impact of enzyme replacement therapy. Heart, 2010, 96, 1915-1919.	2.9	54
30	Effects of exercise training on left ventricular volumes and function in patients with nonischemic cardiomyopathy: Application of magnetic resonance myocardial tagging. American Heart Journal, 2002, 144, 719-725.	2.7	53
31	Novel desmoplakin mutation: juvenile biventricular cardiomyopathy with left ventricular non-compaction and acantholytic palmoplantar keratoderma. Clinical Research in Cardiology, 2011, 100, 1087-1093.	3.3	51
32	Comparison of magnetic resonance imaging and 99mTechnetium-labelled methylene diphosphonate bone scintigraphy in the initial assessment of chronic non-bacterial osteomyelitis of childhood and adolescents. Clinical and Experimental Rheumatology, 2012, 30, 578-82.	0.8	49
33	Management of Spontaneous Pneumothorax and Post-Interventional Pneumothorax: German S3 Guideline. Respiration, 2019, 97, 370-402.	2.6	48
34	Time course of23Na signal intensity after myocardial infarction in humans. Magnetic Resonance in Medicine, 2004, 52, 545-551.	3.0	47
35	Pulmonary fibrosis in youth treated with radioiodine for juvenile thyroid cancer and lung metastases after Chernobyl. European Journal of Nuclear Medicine and Molecular Imaging, 2011, 38, 1683-1690.	6.4	47
36	Diffusion-weighted MRI for detection and differentiation of musculoskeletal tumorous and tumor-like lesions in pediatric patients. World Journal of Pediatrics, 2012, 8, 342-349.	1.8	46

#	Article	IF	CITATIONS
37	Echocardiographic quantification of regional deformation helps to distinguish isolated left ventricular non-compaction from dilated cardiomyopathy. European Journal of Heart Failure, 2012, 14, 155-161.	7.1	45
38	Diffusion-weighted MRI of bone marrow oedema, soft tissue oedema and synovitis in paediatric patients: feasibility and initial experience. Pediatric Rheumatology, 2012, 10, 20.	2.1	45
39	Effects of Exercise Training on Myocardial Energy Metabolism and Ventricular Function Assessed by Quantitative Phosphorus-31 Magnetic Resonance Spectroscopy and Magnetic Resonance Imaging in Dilated Cardiomyopathy. Journal of the American College of Cardiology, 2008, 51, 1883-1891.	2.8	44
40	Optimization of ECG-triggered 3D23Na MRI of the human heart. Magnetic Resonance in Medicine, 2001, 45, 164-166.	3.0	41
41	Fabry disease: Diagnosis and treatment. Kidney International, 2003, 63, S181-S185.	5.2	41
42	Early detection of organ involvement in Fabry disease by biomarker assessment in conjunction with LGE cardiac MRI: results from the SOPHIA study. Molecular Genetics and Metabolism, 2019, 126, 169-182.	1.1	41
43	Auto-SENSE perfusion imaging of the whole human heart. Journal of Magnetic Resonance Imaging, 2003, 18, 702-708.	3.4	40
44	Heart Valve Involvement in Fabry Cardiomyopathy. Ultrasound in Medicine and Biology, 2009, 35, 730-735.	1.5	39
45	Development of a Scoring Tool for Chronic Nonbacterial Osteomyelitis Magnetic Resonance Imaging and Evaluation of its Interrater Reliability. Journal of Rheumatology, 2020, 47, 739-747.	2.0	37
46	Age and gender dependence of human cardiac phosphorus metabolites determined by SLOOP31P MR spectroscopy. Magnetic Resonance in Medicine, 2006, 56, 907-911.	3.0	36
47	Stem cell transplantation for osteopetrosis in patients beyond the age of 5 years. Blood Advances, 2019, 3, 862-868.	5.2	34
48	Absolute quantification of myocardial perfusion under adenosine stress. Magnetic Resonance in Medicine, 2006, 56, 844-849.	3.0	33
49	Myocardial Fibrosis Predicts 10-Year Survival in Patients Undergoing Aortic Valve Replacement. Circulation: Cardiovascular Imaging, 2018, 11, e007131.	2.6	33
50	Cardiac energy metabolism is disturbed in Fabry disease and improves with enzyme replacement therapy using recombinant human galactosidase A. European Journal of Heart Failure, 2011, 13, 278-283.	7.1	32
51	Patterns of serial rib fractures after blunt chest trauma: An analysis of 380 cases. PLoS ONE, 2019, 14, e0224105.	2.5	31
52	Advances in human cardiac ³¹ Pâ€MR spectroscopy: SLOOP and clinical applications. Journal of Magnetic Resonance Imaging, 2001, 13, 521-527.	3.4	30
53	Biochemical cartilage alteration and unexpected signal recovery in T2* mapping observed in ankle joints with mobile MRI during a transcontinental multistage footrace over 4486Âkm. Osteoarthritis and Cartilage, 2014, 22, 1840-1850.	1.3	29
54	Diagnostic Value of Diffusion-Weighted MRI for Tumor Characterization, Differentiation and Monitoring in Pediatric Patients with Neuroblastic Tumors. RoFo Fortschritte Auf Dem Gebiet Der Rontgenstrahlen Und Der Bildgebenden Verfahren, 2017, 189, 640-650.	1.3	29

#	Article	IF	CITATIONS
55	Crossâ€sectional baseline analysis of electrocardiography in a large cohort of patients with untreated Fabry disease. Journal of Inherited Metabolic Disease, 2013, 36, 873-879.	3.6	27
56	A standardized clinical and radiological follow-up of patients with chronic non-bacterial osteomyelitis treated with pamidronate. Clinical and Experimental Rheumatology, 2014, 32, 604-9.	0.8	27
57	Interobserver variability, detection rate, and lesion patterns of 68Ga-PSMA-11-PET/CT in early-stage biochemical recurrence of prostate cancer after radical prostatectomy. European Journal of Nuclear Medicine and Molecular Imaging, 2020, 47, 2339-2347.	6.4	26
58	Effects of exercise training on left ventricular volumes and function in patients with nonischemic cardiomyopathy: Application of magnetic resonance myocardial tagging. American Heart Journal, 2002, 144, 719-725.	2.7	25
59	Abscess-forming lymphadenopathy and osteomyelitis in children with Bartonella henselae infection. Journal of Medical Microbiology, 2008, 57, 519-524.	1.8	25
60	Imaging pediatric gastrointestinal stromal tumor (GIST). Journal of Pediatric Surgery, 2018, 53, 1862-1870.	1.6	25
61	Ultrasound 2020 – Diagnostics & Therapy: On the Way to Multimodal Ultrasound: Contrast-Enhanced Ultrasound (CEUS), Microvascular Doppler Techniques, Fusion Imaging, Sonoelastography, Interventional Sonography. RoFo Fortschritte Auf Dem Gebiet Der Rontgenstrahlen Und Der Bildgebenden Verfahren, 2021, 193, 23-32.	1.3	25
62	Diffusion-weighted MRI of abscess formations in children and young adults. World Journal of Pediatrics, 2012, 8, 229-234.	1.8	24
63	Management of Spontaneous Pneumothorax and Postinterventional Pneumothorax: German S3-Guideline. Zentralblatt Fur Chirurgie, 2018, 143, S12-S43.	0.3	24
64	Cardiac and skeletal muscle involvement in myotonic dystrophy type 2 (DM2): A quantitative31P-MRS and MRI study. Muscle and Nerve, 2004, 30, 636-644.	2.2	23
65	Tei Index in Fabry Disease. Journal of the American Society of Echocardiography, 2011, 24, 1026-1032.	2.8	23
66	Impact of Regional Left Ventricular Function on Outcome for Patients with AL Amyloidosis. PLoS ONE, 2013, 8, e56923.	2.5	23
67	Interdisciplinary approach towards female patients with Fabry disease. European Journal of Clinical Investigation, 2012, 42, 455-462.	3.4	22
68	Sodium T2* relaxation times in human heart muscle. Journal of Magnetic Resonance Imaging, 2002, 15, 215-218.	3.4	20
69	Magnetic Resonance Imaging in Child Abuse. Journal of Child Neurology, 2007, 22, 170-175.	1.4	20
70	Quantitative contrastâ€enhanced perfusion measurements of the human lung using the prebolus approach. Journal of Magnetic Resonance Imaging, 2009, 30, 104-111.	3.4	20
71	Lung imaging under freeâ€breathing conditions. Magnetic Resonance in Medicine, 2009, 61, 723-727.	3.0	20
72	Differentiation Between Fresh and Old Left Ventricular Thrombi by Deformation Imaging. Circulation: Cardiovascular Imaging, 2012, 5, 667-675.	2.6	20

#	Article	IF	CITATIONS
73	Spongious Hypertrophic Cardiomyopathy in Patients With Mutations in the Four-and-a-Half LIM Domain 1 Gene. Circulation: Cardiovascular Genetics, 2012, 5, 490-502.	5.1	20
74	Breath-hold 3D MR coronary angiography with a new intravascular contrast agent (feruglose)—first clinical experiences. Magnetic Resonance Imaging, 2001, 19, 201-205.	1.8	19
75	Cardiac spectroscopy: techniques, indications and clinical results. European Radiology, 2004, 14, 1034-1047.	4.5	19
76	Quantification of inflammatory activity in patients with Crohn's disease using diffusion weighted imaging (DWI) in MR enteroclysis and MR enterography. Acta Radiologica, 2017, 58, 264-271.	1.1	19
77	Structured Reporting in Cross-Sectional Imaging of the Heart: Reporting Templates for CMR Imaging of Cardiomyopathies (Myocarditis, Dilated Cardiomyopathy, Hypertrophic Cardiomyopathy,) Tj ETQq1 1 0.784 Der Rontgenstrahlen Und Der Bildgebenden Verfahren, 2020, 192, 27-37.	314 rgBT /C	Dverlock 10 Tf
78	MR-based analysis of regional cardiac function in relation to cellular integrity in Fabry disease. International Journal of Cardiology, 2012, 160, 53-58.	1.7	18
79	Imaging in non-bacterial osteomyelitis in children and adolescents: diagnosis, differential diagnosis and follow-up—an educational review based on a literature survey and own clinical experiences. Insights Into Imaging, 2021, 12, 113.	3.4	18
80	Cine MR imaging after myocardial infarctionassessment and follow-up of regional and global left ventricular function. International Journal of Cardiovascular Imaging, 1999, 15, 435-440.	0.6	17
81	Time course of contrast enhancement patterns after Gd-BOPTA in correlation to myocardial infarction and viability: A feasibility study. Journal of Magnetic Resonance Imaging, 2001, 14, 789-794.	3.4	17
82	Free breathing cardiac real-time cine MR without ECG triggering. International Journal of Cardiology, 2010, 145, 380-382.	1.7	17
83	Comparison of intravascular and extracellular contrast media for absolute quantification of myocardial restâ€perfusion using highâ€resolution MRI. Journal of Magnetic Resonance Imaging, 2011, 33, 1047-1051.	3.4	17
84	Dual Energy Computed Tomography in Musculoskeletal Imaging, with Focus on Fragility Fractures of the Pelvis. Zeitschrift Fur Orthopadie Und Unfallchirurgie, 2017, 155, 708-715.	0.7	17
85	Detection of myocardial infarctions by acquisition-weighted31P-MR spectroscopy in humans. Journal of Magnetic Resonance Imaging, 2004, 20, 798-802.	3.4	16
86	Comparison of different contrast agents and doses for quantitative MR myocardial perfusion imaging. Journal of Magnetic Resonance Imaging, 2008, 28, 382-389.	3.4	16
87	Pitfalls in diagnostics of hip pain: osteoid osteoma and osteoblastoma. Rheumatology International, 2010, 30, 395-400.	3.0	16
88	Cardiac catheter ablation under real-time magnetic resonance guidance. European Heart Journal, 2012, 33, 1977-1977.	2.2	16
89	Potential role of CT-textural features for differentiation between viral interstitial pneumonias, pneumocystis jirovecii pneumonia and diffuse alveolar hemorrhage in early stages of disease: a proof of principle. BMC Medical Imaging, 2019, 19, 39.	2.7	16
90	Correction for partial volume errors in MR heart perfusion imaging. Magnetic Resonance in Medicine, 2004, 51, 848-852.	3.0	15

#	Article	IF	CITATIONS
91	Popliteal Cysts in Paediatric Patients: Clinical Characteristics and Imaging Features on Ultrasound and MRI. Arthritis, 2011, 2011, 1-7.	2.0	15
92	Multiparametric MRI of the prostate with three functional techniques in patients with PSA elevation before initial TRUS-guided biopsy. British Journal of Radiology, 2015, 88, 20150422.	2.2	15
93	First experiences with Lu-177 PSMA therapy in combination with Pembrolizumab or after pretreatment with Olaparib in single patients. Journal of Nuclear Medicine, 2021, 62, jnumed.120.249029.	5.0	15
94	Characteristic morphological patterns within adolescent idiopathic scoliosis may be explained by mechanical loading. European Spine Journal, 2018, 27, 2184-2191.	2.2	14
95	Simple liver cysts and cystoid lesions in hepatic alveolar echinococcosis: a retrospective cohort study with Hounsfield analysis. Parasite, 2019, 26, 54.	2.0	14
96	Hepatic alveolar echinococcosis: correlation between computed tomography morphology and inflammatory activity in positron emission tomography. Scientific Reports, 2020, 10, 11808.	3.3	14
97	Deep Neural Networks and Machine Learning Radiomics Modelling for Prediction of Relapse in Mantle Cell Lymphoma. Cancers, 2022, 14, 2008.	3.7	14
98	Functional and Metabolic Recovery of the Right Ventricle During Bosentan Therapy in Idiopathic Pulmonary Arterial Hypertension. Journal of Cardiovascular Magnetic Resonance, 2005, 7, 853-854.	3.3	13
99	Follow-up MR imaging of PI-RADS 3 and PI-RADS 4 prostate lesions. Clinical Imaging, 2017, 43, 64-68.	1.5	13
100	MRI Cartilage Assessment of the Subtalar and Midtarsal Joints During a Transcontinental Ultramarathon – New Insights into Human Locomotion. International Journal of Sports Medicine, 2018, 39, 37-49.	1.7	13
101	<scp>2D</scp> Ultrashort Echoâ€Time Functional Lung Imaging. Journal of Magnetic Resonance Imaging, 2020, 52, 1637-1644.	3.4	13
102	Two Novel Compound Heterozygous Mutations in the TRAPPC9 Gene Reveal a Connection of Non-syndromic Intellectual Disability and Autism Spectrum Disorder. Frontiers in Genetics, 2020, 11, 972.	2.3	13
103	Absolute quantification of high energy phosphate metabolites in normal, hypertrophied and failing human myocardium. Magnetic Resonance Materials in Physics, Biology, and Medicine, 2000, 11, 73-74.	2.0	12
104	Evaluation of sodium T1 relaxation times in human heart. Journal of Magnetic Resonance Imaging, 2003, 17, 726-729.	3.4	12
105	Myocardial involvement and deformation abnormalities in idiopathic inflammatory myopathy assessed by CMR feature tracking. International Journal of Cardiovascular Imaging, 2021, 37, 597-603.	1.5	12
106	Non-Invasive Functional and Biochemical Assessment of Mitoxantrone Cardiotoxicity in Patients with Multiple Sclerosis. Journal of Cardiovascular Pharmacology, 2003, 42, 680-687.	1.9	11
107	Diagnostic value of semi-quantitative and quantitative analysis of functional parameters in multiparametric MRI of the prostate. British Journal of Radiology, 2017, 90, 20170067.	2.2	11
108	Cardiac structure and function in response to a multi-stage marathon over 4486 km. European Journal of Preventive Cardiology, 2021, 28, 1102-1109.	1.8	11

IF # ARTICLE CITATIONS A mobile MRI field study of the biochemical cartilage reaction of the knee joint during a 4,486 km transcontinental multistage ultra-marathon using T2* mapping. Scientific Reports, 2020, 10, 8157. Dental and Maxillofacial Cone Beam CTâ€"High Number of Incidental Findings and Their Impact on 110 2.6 11 Follow-Up and Therapy Management. Diagnostics, 2022, 12, 1036. Large, segmental, circular vascular malformation of the small intestine (in a female toddler with) Tj ETQq1 1 0.784314 rgBT /Qxerlock Quantitative DWI predicts event-free survival in children with neuroblastic tumours: preliminary 112 3.4 10 findings from a retrospective cohort study. European Radiology Experimental, 2019, 3, 6. First successful transcatheter double valve replacement from a transapical access and nine-month 3.2 follow-up. EuroIntervention, 2017, 12, 1645-1648. The Value of APTw CEST MRI in Routine Clinical Assessment of Human Brain Tumor Patients at 3T. 114 2.6 10 Diagnostics, 2022, 12, 490. Hemodynamic Assessment of Severe Aortic Stenosis. Investigative Radiology, 2011, 46, 1-10. 6.2 Hit the mark with diffusion-weighted imaging: metastases of rhabdomyosarcoma to the extraocular 116 1.7 9 eye muscles. BMC Pediatrics, 2014, 14, 57. Combining Computed Tomography and Histology Leads to an Evolutionary Concept of Hepatic Alveolar Echinococcosis. Pathogens, 2020, 9, 634. 2.8 Caffeine impairs intramuscular energy balance in patients susceptible to malignant hyperthermia. 118 2.2 8 Muscle and Nerve, 2003, 28, 353-358. Intracardial dislocation of a cranio-peritoneal shunt in a 6-year-old boy. Clinical Research in 119 3.3 Cardiology, 2010, 99, 677-678. Characterization of a calcified intra-cardiac pseudocyst of the mitral valve by magnetic resonance 120 1.7 8 imaging including T1 and T2 mapping. BMC Cardiovascular Disorders, 2014, 14, 11. Iterative scatter correction for grid-less skeletal radiography allows improved image quality equal to an antiscatter grid in adjunct with dose reduction: a visual grading study of 20 body donors. Acta Radiologica, 2019, 60, 735-741. 1.1 Short-Interval, Low-Dose Peptide Receptor Radionuclide Therapy in Combination with PD-1 Checkpoint Immunotherapy Induces Remission in Immunocompromised Patients with Metastatic Merkel Cell 122 4.5 8 Carcinoma. Pharmaceutics, 2022, 14, 1466. Extent of size, shape and systolic variability of the left ventricular outflow tract in aortic stenosis 1.8 determined by phase-contrast MRI. Magnetic Resonance Imaging, 2018, 45, 58-65. Shape Modification is Common in Woven EndoBridge–Treated Intracranial Aneurysms: A Longitudinal 124 2.4 7 Quantitative Analysis Study. American Journal of Neuroradiology, 2020, 41, 1652-1656. Changes of Radiation Treatment Concept Based on 68Ga-PSMA-11-PET/CT in Early PSA-Recurrences After 2.8 Radical Prostatectomy. Frontiers in Oncology, 2021, 11, 665304.

126 Clubbing due to Peripheral Hypervascularization. Circulation, 2001, 104, 2503-2503.

1.6 6

MEINRAD BEER

#	Article	IF	CITATIONS
127	Osteoarticular infection by Candida albicans in an infant with cystic fibrosis. Journal of Medical Microbiology, 2011, 60, 1542-1545.	1.8	6
128	Reducing the Emission of X-Ray Contrast Agents to the Environment: Decentralized Collection of Urine Bags and Its Acceptance. Gaia, 2018, 27, 147-155.	0.7	6
129	Size-adjusted muscle power and muscle metabolism in patients with cystic fibrosis are equal to healthy controls $\hat{a} \in \hat{a}$ case control study. BMC Pulmonary Medicine, 2019, 19, 269.	2.0	6
130	Pathognomonic imaging signs in abdominal radiology. Abdominal Radiology, 2020, 45, 576-586.	2.1	6
131	Olecranon fractures in children: treatment of a rare entity. European Journal of Trauma and Emergency Surgery, 2022, 48, 3429-3437.	1.7	6
132	Vestibular Nerve Atrophy After Vestibular Neuritis – Results from a Prospective High-Resolution MRI Study. RoFo Fortschritte Auf Dem Gebiet Der Rontgenstrahlen Und Der Bildgebenden Verfahren, 2020, 192, 854-861.	1.3	6
133	Morphological patterns of the rib cage and lung in the healthy and adolescent idiopathic scoliosis. Journal of Anatomy, 2022, 240, 120-130.	1.5	6
134	Pre-race determinants influencing performance and finishing of a transcontinental 4486-km ultramarathon. Journal of Sports Medicine and Physical Fitness, 2019, 59, 1608-1621.	0.7	6
135	Colonic Opacification in a Patient With End-Stage Kidney Disease. Gastroenterology, 2010, 139, e8-e9.	1.3	5
136	Acquisition-weighted chemical shift imaging improves SLOOP quantification of human cardiac phosphorus metabolites. Zeitschrift Fur Medizinische Physik, 2014, 24, 49-54.	1.5	5
137	Evaluation of the Value of Contrast-Enhanced Ultrasound (CEUS) within Radiology Departments in Germany. RoFo Fortschritte Auf Dem Gebiet Der Rontgenstrahlen Und Der Bildgebenden Verfahren, 2017, 189, 748-759.	1.3	5
138	Radiological Diagnosis of Soft Tissue Tumors in Adults: MRI Imaging of Selected Entities Delineating Benign and Malignant Tumors. RoFo Fortschritte Auf Dem Gebiet Der Rontgenstrahlen Und Der Bildgebenden Verfahren, 2019, 191, 323-332.	1.3	5
139	Cardiac involvement in a crossâ€ s ectional cohort of myotonic dystrophies and other skeletal myopathies. ESC Heart Failure, 2020, 7, 1900-1908.	3.1	5
140	The Effect of Multi-Parametric Magnetic Resonance Imaging in Standard of Care for Nonalcoholic Fatty Liver Disease: Protocol for a Randomized Control Trial. JMIR Research Protocols, 2020, 9, e19189.	1.0	5
141	T2*-Mapping of Knee Cartilage in Response to Mechanical Loading in Alpine Skiing: A Feasibility Study. Diagnostics, 2022, 12, 1391.	2.6	5
142	SNR-optimized myocardial perfusion imaging using parallel acquisition for effective density-weighted saturation recovery imaging. Magnetic Resonance Imaging, 2010, 28, 341-350.	1.8	4
143	Density weighted turbo spin echo imaging. Journal of Magnetic Resonance Imaging, 2013, 37, 965-973.	3.4	4
144	Improvement of image quality applying iterative scatter correction for grid-less skeletal radiography in trauma room setting. Acta Radiologica, 2020, 61, 768-775.	1.1	4

#	Article	lF	CITATIONS
145	Liver Iron Content Determination Using a Volumetric Breathâ€Hold Gradientâ€Echo Sequence With Inâ€Line <scp>R₂</scp> * Calculation. Journal of Magnetic Resonance Imaging, 2020, 52, 1550-1556.	3.4	4
146	Accelerated model-based quantitative diffusion MRI: A feasibility study for musculoskeletal application. Zeitschrift Fur Medizinische Physik, 2022, 32, 240-247.	1.5	4
147	Relaxation-weighted ²³ Na magnetic resonance imaging maps regional patterns of abnormal sodium concentrations in amyotrophic lateral sclerosis. Therapeutic Advances in Chronic Disease, 2022, 13, 204062232211094.	2.5	4
148	Assessment of myocardial viability by31P-MR-spectroscopy and23Na-MR imaging. Magnetic Resonance Materials in Physics, Biology, and Medicine, 2000, 11, 44-46.	2.0	3
149	Different Reconstruction Intervals for Exclusion of Coronary Artery Calcifications by Retrospectively Gated MDCT. American Journal of Roentgenology, 2006, 186, 193-197.	2.2	3
150	Energetic differences between viable and non-viable myocardium in patients with recent myocardial infarction are not an effect of differences in wall thinning— a multivoxel 31P-MR-spectroscopy and MRI study. European Radiology, 2007, 17, 1275-1283.	4.5	3
151	Frequency and Diagnostic Implications of Image Artifacts by Eye-Lens Shielding in Head CT. American Journal of Roentgenology, 2019, 212, 607-613.	2.2	3
152	Improving resolution of head and neck CTA using the small x-ray tube focal spot. Neuroradiology, 2019, 61, 953-956.	2.2	3
153	Long distance running – Can bioprofiling predict success in endurance athletes?. Medical Hypotheses, 2021, 146, 110474.	1.5	3
154	MRI-guided ablation of wide complex tachycardia in a univentricular heart. World Journal of Cardiology, 2012, 4, 260.	1.5	3
155	Evaluation of an elective ultrasound course for medical students. Clinical Anatomy, 2022, 35, 354-358.	2.7	3
156	Ex Vivo High-Resolution Magic Angle Spinning (HRMAS) 1H NMR Spectroscopy for Early Prostate Cancer Detection. Cancers, 2022, 14, 2162.	3.7	3
157	Moyamoya disease associated with pediatric pulmonary hypertension—a case report. Cardiovascular Diagnosis and Therapy, 2021, 11, 1052-1056.	1.7	2
158	Impact of cardiac magnet resonance imaging on management of ventricular septal rupture after acute myocardial infarction. World Journal of Cardiology, 2013, 5, 151.	1.5	2
159	Assessment of myocardial viability by 31P-MR-spectroscopy and 23Na-MR imaging. Magnetic Resonance Materials in Physics, Biology, and Medicine, 2000, 11, 44-46.	2.0	1
160	Multi-slice cardiac computed tomography reveals anomalous origin of the right coronary artery between the great arteries. International Journal of Cardiology, 2007, 119, e77-e78.	1.7	1
161	Acute Muscle Trauma due to Overexercise in an Otherwise Healthy Patient with Cystic Fibrosis. Case Reports in Pediatrics, 2012, 2012, 1-4.	0.4	1
162	Atypical hypertrophic cardiomyopathy of the left lateral wall leading to ventricular tachycardia. European Heart Journal, 2014, 35, 548-548.	2.2	1

#	Article	IF	CITATIONS
163	Reproducibility of manual and semi-automated late enhancement quantification in patients with Fabry disease. Acta Radiologica, 2014, 55, 155-160.	1.1	1
164	Prediction of response to endobronchial coiling based on morphologic emphysema characterization of the lung lobe to be treated and the ipsilateral non-treated lobe as well as on functional computed tomography-data: correlation with clinical and pulmonary function. Journal of Thoracic Disease, 2019, 11, 93-102.	1.4	1
165	18F-FDG-PET/MR in Alveolar Echinococcosis: Multiparametric Imaging in a Real-World Setting. Pathogens, 2022, 11, 348.	2.8	1
166	Non-Uniform Self-Gating in 2D Lung Imaging. Frontiers in Physics, 2022, 10, .	2.1	1
167	Sonography in Childhood and Adolescence for General Radiologists – More Possibilities Than Expected RoFo Fortschritte Auf Dem Gebiet Der Rontgenstrahlen Und Der Bildgebenden Verfahren, 2021, , .	1.3	1
168	Accurate metabolic images of the human myocardium by means of ³¹ P magnetic resonance chemical shift imaging with spatial saturation pulses. Concepts in Magnetic Resonance Part A: Bridging Education and Research, 2013, 42, 187-195.	0.5	0
169	Correct positioning of central venous catheters with ECG guidance in paediatric patients. European Journal of Anaesthesiology, 2016, 33, 550-552.	1.7	0
170	Non-invasive determination of pressure recovery by cardiac MRI and echocardiography in patients with severe aortic stenosis: short and long-term outcome prediction. Journal of International Medical Research, 2020, 48, 030006052095470.	1.0	0
171	Long term evolution of magnetic resonance imaging characteristics in a case of atypical left lateral wall hypertrophic cardiomyopathy. World Journal of Cardiology, 2015, 7, 357.	1.5	0